

RESEARCH ARTICLE

10.1002/2015GB005097

Key Points:

- Storms significantly contribute to annual nitrate budgets
- Poststorm inertial currents produce spikes of high diffusive nitrate flux
- Their impact on nitrate supply is low compared to wind mixing during a storm

Supporting Information:

- Text S1
- Figure S1

Correspondence to:

A. Rumyantseva,
asr1g12@soton.ac.uk

Citation:

Rumyantseva, A., N. Lucas, T. Rippeth, A. Martin, S. C. Painter, T. J. Boyd, and S. Henson (2015), Ocean nutrient pathways associated with the passage of a storm, *Global Biogeochem. Cycles*, 29, 1179–1189, doi:10.1002/2015GB005097.

Received 16 JAN 2015

Accepted 13 JUL 2015

Accepted article online 16 JUL 2015

Published online 14 AUG 2015

©2015. The Authors.

This is an open access article under the terms of the Creative Commons Attribution License, which permits use, distribution and reproduction in any medium, provided the original work is properly cited.

Ocean nutrient pathways associated with the passage of a storm

Anna Rumyantseva^{1,2}, Natasha Lucas³, Tom Rippeth³, Adrian Martin¹, Stuart C. Painter¹, Timothy J. Boyd⁴, and Stephanie Henson¹

¹National Oceanography Centre, Southampton, UK, ²Ocean and Earth Science, University of Southampton, Southampton, UK, ³School of Ocean Sciences, Bangor University, Menai Bridge, UK, ⁴The Scottish Association for Marine Science, Scottish Marine Institute, Argyll, UK

Abstract Storms that affect ocean surface layer dynamics and primary production are a frequent occurrence in the open North Atlantic Ocean. In this study we use an interdisciplinary data set collected in the region to quantify nutrient supply by two pathways associated with a storm event: entrainment of nutrients during a period of high wind forcing and subsequent shear spiking at the pycnocline due to interactions of storm-generated inertial currents with wind. The poststorm increase in surface layer nitrate (by $\sim 20 \text{ mmol m}^{-2}$) was predominantly driven by the first pathway: nutrient intrusion during the storm. Alignment of poststorm inertial currents and surface wind stress caused shear instabilities at the ocean pycnocline, forming the second pathway for nutrient transport into the euphotic zone. During the alignment period, pulses of high-turbulence nitrate flux through the pycnocline (up to $1 \text{ mmol m}^{-2} \text{ d}^{-1}$; approximately 25 times higher than the background flux) were detected. However, the impact of the poststorm supply was an order of magnitude lower than during the storm due to the short duration of the pulses. Cumulatively, the storm passage was equivalent to 2.5–5% of the nitrate supplied by winter convection and had a significant effect compared to previously reported (sub)mesoscale dynamics in the region. As storms occur frequently, they can form an important component in local nutrient budgets.

1. Introduction

Primary production in the temperate and subpolar North Atlantic Ocean plays a crucial role in the global carbon cycle [Sabine *et al.*, 2004]. However, the precise physical mechanisms that supply nutrients to support observed levels of annual primary production and the relative importance of these mechanisms are still under debate [McGillicuddy *et al.*, 2003; Oschlies, 2002a]. Many studies have focused on the impact of mesoscale and submesoscale dynamics [Lévy *et al.*, 2012; Martin and Richards, 2001; McGillicuddy *et al.*, 1998], the transport of nutrients by major ocean currents [Pelegri *et al.*, 2006], and winter convection [Williams *et al.*, 2000] as pathways for nutrient supply to support primary production. However, less attention has been given to nutrient fluxes associated with the passage of storms.

In temperate and high-latitude oceans, strong wind forcing can be particularly important during the postspring bloom period when the surface ocean is nitrate-depleted and a well-established pycnocline inhibits the upward flux of nutrients to the euphotic zone. Under these conditions primary production is predominantly fuelled by regenerated forms of nitrogen such as ammonium and urea unless physical resupply of nutrients occurs. Satellite observations of episodic storm events in summer and autumn have been linked to subsequent phytoplankton increases in otherwise nutrient-limited conditions [Babin *et al.*, 2004; Son *et al.*, 2006; Wu *et al.*, 2008].

The passage of a storm can initiate transport of nitrate from the ocean interior to the euphotic zone in several ways. The classic interpretation of the wind-induced nutrient supply is that enhanced vertical mixing during strong wind forcing breaks down vertical stratification, erodes the pycnocline, and entrains nutrient-rich deeper water into the mixed layer [Findlay *et al.*, 2006; Marra *et al.*, 1990].

Another pathway, rarely documented in observational data, is associated with the interaction between wind stress and surface layer currents, resulting in an intermittent pulsed nutrient flux through the pycnocline [Rippeth *et al.*, 2009]. Abrupt changes in wind stress induce near-inertial oscillations [Pollard, 1980] that can last for several days before decaying. When the directions of wind stress and these near-inertial oscillations

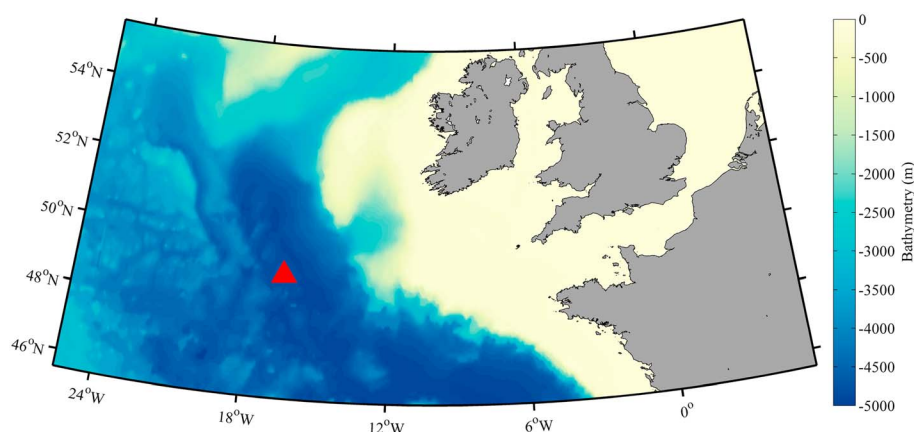


Figure 1. Bathymetry map of the northeast Atlantic Ocean showing the location of the sampling site during D381 cruise.

align, enhanced shear production can be sufficient to generate turbulence through Kelvin-Helmholtz instabilities such that the energy dissipation rate across the pycnocline can increase by an order of magnitude [Lenn *et al.*, 2011; Rippeth *et al.*, 2005]. This mechanism, referred to as shear spiking, has been shown to produce near-inertial pulses of high-turbulence nitrate flux across the pycnocline (compared to typically low background levels) by previous interdisciplinary studies in temperate shelf seas [Rippeth *et al.*, 2009; Williams *et al.*, 2013]. Shear spiking can supply nutrients during high wind forcing as well as in the poststorm period when inertial currents persist in the water column. Open ocean in situ observations of this process have been limited since they require coincident measurements of ocean microstructure and currents over several days.

This paper presents direct observations of the flux of nutrients to the surface layer resulting from the passage of an autumn extratropical storm in the open North Atlantic Ocean. Specifically, we quantify the nutrient flux during the storm and additional supply of nutrients after the storm passage associated with the shear-spiking mechanism. The efficiency of the overall storm-induced nutrient supply is compared to other more widely recognized mechanisms in order to assess the storm's contribution to the nutrient budget of the North Atlantic Ocean.

2. Data and Methods

2.1. Observational Study

This study is based on an interdisciplinary data set collected aboard RRS Discovery (cruise D381) in the framework of the UK Natural Environment Research Council (NERC) OSMOSIS (Ocean Surface Mixing Ocean Submesoscale Interaction Study) project. The sampling campaign was carried out 40 km southeast of the Porcupine Abyssal Plain (PAP) Sustained Observatory (49°N, 16.5°W; Figure 1 [Lampitt *et al.*, 2010]), from 31 August to 1 October 2012 (year days 244 to 275).

The observations (Figure 2) included turbulence measurements using a MSS90 microstructure profiler, standard CTD (conductivity-temperature-depth) profiling using a SeaBird 911, current measurements using a vessel-mounted RDI "Ocean Surveyor" 75 kHz ADCP (acoustic Doppler current profiler), and underway water samples from the nontoxic seawater supply (approximate intake depth of 5 m) and surface meteorology. Additionally, two Seagliders surveyed the area for a year (September 2012 to September 2013), equipped with an unpumped conductivity-temperature sensor, a Wetlabs ECOpuck (including chlorophyll *a*, hereafter chl *a*, fluorescence sensor), and a spherical photosynthetically available radiation sensor, providing vertical profiles of biophysical properties of the ocean boundary layer over the duration of the cruise and beyond. Details of Seaglider data processing and calibration are presented in the supporting information. Sampling for inorganic nutrient concentrations was undertaken from both CTD casts and the underway nontoxic seawater supply. Analysis of nitrate + nitrite (hereafter nitrate) concentrations was conducted using a Skalar-Sanplus autoanalyzer and the method described by Kirkwood [1996].

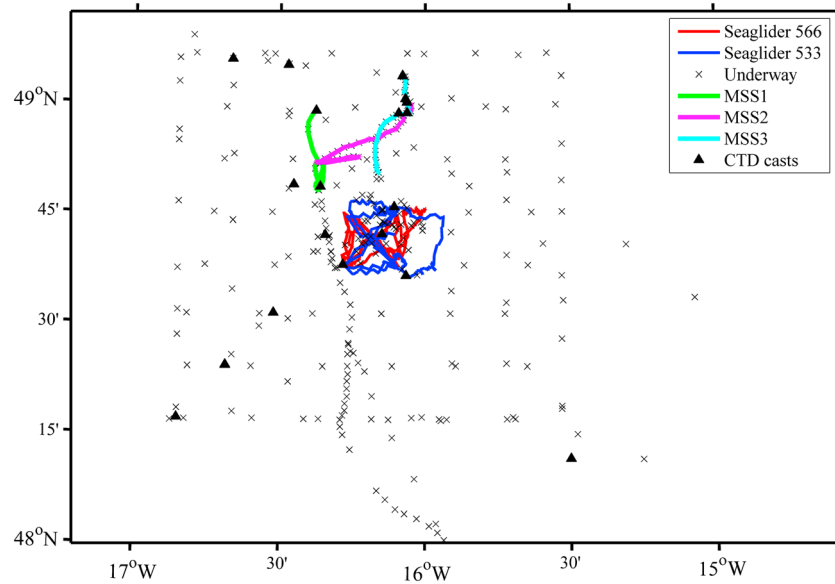


Figure 2. Sampling map for cruise D381: Seagliders 566 and 533 (red and blue lines, respectively); underway samples (grey crosses); three series of turbulence measurements: MSS1 (green line), MSS2 (magenta line), and MSS3 (light blue line); CTD casts (black triangles).

2.2. Turbulent Nitrate Flux Calculations

Estimates of the nitrate flux through the pycnocline were based on vertical profiles of turbulent kinetic energy dissipation. During the course of the cruise, three series of turbulence measurements extending to a depth of ~200 m were conducted:

MSS1 From year day 260.9 to 262.5 (238 profiles)

MSS2 From year day 265.3 to 266.5 day of year (202 profiles)

MSS3 From year day 270.8 to 272.0 day of year (175 profiles)

Estimates of the turbulent kinetic energy dissipation rate (ϵ) were obtained from raw shear data using the MSSPRO software standard processing sequence. All data from the MSS probe for each profile were averaged into 1 m bins. For each bin the eddy diffusivity was calculated from the energy dissipation rate following *Osborn* [1980]:

$$K = 0.2 \frac{\epsilon}{N^2} \quad (1)$$

where K is the eddy diffusivity and N is the buoyancy frequency. Subsequently, nitrate flux at depth d can be defined through multiplying the diffusivity term by the local nitrate gradient:

$$F = K \left. \frac{\partial \text{NO}_3}{\partial z} \right|_{z=d} \quad (2)$$

where NO_3 is the nitrate concentration. Following *Sharples et al.* [2007], CTD bottle data were used to derive a nitrate-density relation and obtain vertically resolved profiles of $\frac{\partial \text{NO}_3}{\partial z}$. We found a strong linear relationship between density and nitrate (Figure 3a; $R^2 = 0.88$, $P < 0.0001$), allowing nitrate gradients to be represented in equation (2) as $m \frac{\partial \rho}{\partial z}$, where ρ is the density measured by the microstructure profiler and $m = 2.4 \pm 0.1 \text{ mmol N m}^{-3} (\text{kg m}^{-3})^{-1}$ is the nitrate-density gradient. Representative vertical profiles of density and nitrate are shown in Figure 3b. Uncertainty associated with the estimated nitrate-density gradient (~5%) is negligible compared to uncertainties associated with eddy diffusivity measurements in the ocean; therefore, $m = 2.4 \text{ mmol N m}^{-3} (\text{kg m}^{-3})^{-1}$ was used in the further calculations of the nitrate flux.

2.3. Bulk Shear Estimation and Theoretical Model

Episodic bursts of shear, attributed to alignment and interaction of shear and wind forcing, have been quantified for the open ocean using a modified shear production model as described in *Brannigan et al.* [2013], which is

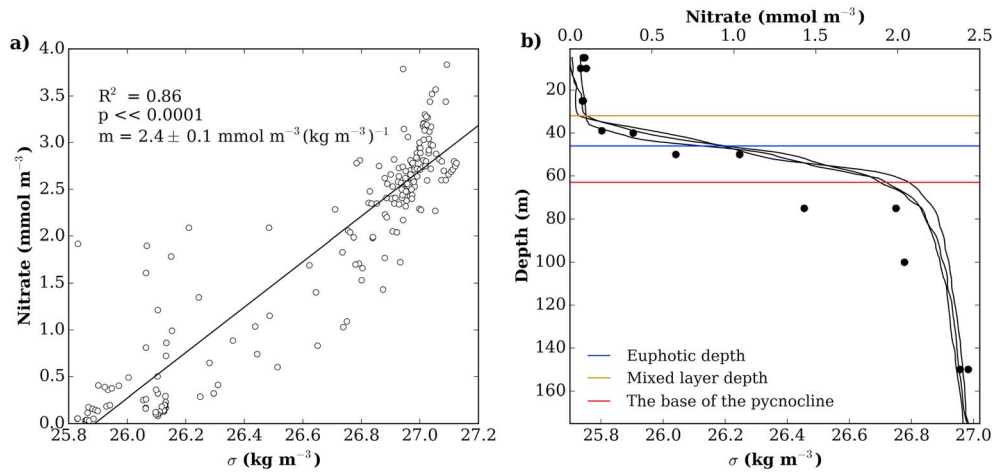


Figure 3. (a) The nitrate-density relationship within the pycnocline for all CTD casts collected during D381 cruise. m is the slope of the linear regression $\pm 95\%$ confidence intervals. (b) CTD profiles collected close in time (decimal days 264–265) illustrating vertical distribution of density (black lines) and nitrate (black circles) during D381 cruise. The horizontal lines on the plot indicate the corresponding mean values of the euphotic depth (blue), mixed layer depth (yellow), and the base of the pycnocline (red).

adapted from a prognostic expression derived from one-dimensional momentum equations for stratified tidal shelf seas [Burchard and Rippeth, 2009]. In this model the authors define a two-layer damped-slab model, with the relationship between velocity and bulk shear as

$$\vec{S} = \frac{\vec{u}_H - \vec{u}_L}{h_s} \tag{3}$$

where \vec{u}_H and \vec{u}_L are the velocities in the mixed layer H and lower layer L , respectively, and h_s is the distance between the centers of mass of these layers, separated by a pycnocline layer. In this work we define a variable pycnocline as the layer between the mixed layer depth (MLD) and the base of the pycnocline. The definition of MLD was based on *de Boyer Montégut et al.* [2004] and calculated using a change in temperature of 0.2°C relative to the value at 10 m depth. The base of the pycnocline was determined following *Johnston and Rudnick* [2009], as the depth below the mean mixed layer depth of the deepest isopycnal within one standard deviation of the mean mixed layer depth. In this model the lower layer was defined as a 48 m deep layer immediately below the base of the pycnocline, as this limit was large enough to capture the slab dynamics while falling within the ADCP bin resolution.

Following the derivation in *Brannigan et al.* [2013] and using the slab layers defined here, a relationship for the rate of change of bulk shear squared with respect to time is obtained with the production or destruction of shear being brought about by the relative orientation between wind and bulk shear directions:

$$\frac{\partial S^2}{\partial t} = 2 \left(\frac{\vec{S} \cdot \vec{T}_w}{h_s \rho H} - c_i \frac{h_s}{H} |S^3| \right) \tag{4}$$

where c_i is the drag coefficient, \vec{T}_w is the wind stress, and ρ is a reference density. When the dot product is greater than zero (i.e., $\cos(\vec{S}, \vec{T}_w) > 0$), directions of wind and shear are favorable for enhanced shear production. If the wind magnitude is constant, the maximum shear production occurs when \vec{S} and \vec{T}_w align.

3. Results

3.1. Surface Dynamics

Atmospheric conditions during the cruise were characterized by a storm that started on day 268 (24 September 2012) and continued until day 270.6 (27 September 2012) with typical wind forcing $0.3\text{--}0.4 \text{ N m}^{-2}$ (Figure 4a). Underway nutrient and Seaglider chl a fluorescence data suggest a biochemical response to the storm event (Figures 4c and 4d). The surface nitrate concentration after the storm had increased from $<0.1 \text{ mmol N m}^{-3}$

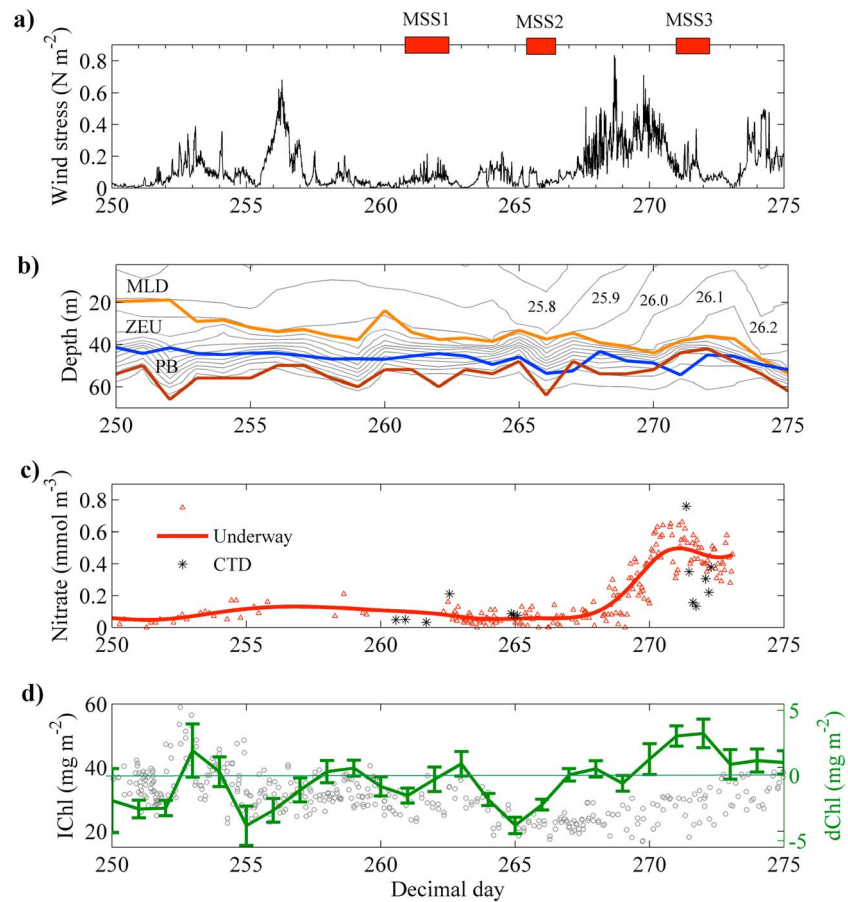


Figure 4. Wind and biophysical data collected during cruise D381. (a) The 10 min averaged wind stress was calculated as in *Large et al.* [1995] using wind speed data measured by the weather station on RRS Discovery. The red rectangles at the top show the timing of three series of turbulence measurements: MSS1, MSS2, and MSS3. (b) The Seagliders time series of isopycnal surfaces (grey lines), mixed layer depth (MLD) defined as a temperature differential of 0.2°C from 10 m depth (orange line), euphotic depth (ZEU; blue line; details of the calculations are presented in the supporting information), and the base of the pycnocline (PB; brown line). (c) Surface nitrate variability during the cruise: the red triangles are the surface (~5 m) nitrate concentrations from the ship underway system, and the red solid line is the fitted smooth spline. The black stars represent the mean nitrate concentration within the mixed layer estimated from CTD casts. (d) Integrated chl *a* (IChl; grey circles) and daily change in integrated chl *a* (dChl; green line; Seagliders data).

to almost $0.6 \text{ mmol N m}^{-3}$. The time series of change in integrated chl *a* (dChl) showed that replenishment of the surface layer with nutrients was coincident with increased phytoplankton stocks (i.e., $\text{dChl} > 0$). The prestorm period was characterized by mostly negative dChl (Figure 4d) due to lack of nutrients within the mixed layer (Figure 3b) and therefore decreasing phytoplankton growth rate representative of typical conditions in the high-latitude North Atlantic Ocean over the postspring bloom period.

3.2. Nutrient Supply During the Storm

The ability of Seagliders to obtain data under challenging weather conditions allowed them to capture the changes in the surface layer dynamics throughout the storm event. The data showed that vertical mixing during the associated strong wind forcing introduced significant changes in the upper ocean density structure: an increase in surface density from $\sim 25.8 \text{ kg m}^{-3}$ to $\sim 26.1 \text{ kg m}^{-3}$ and erosion of the pycnocline (Figure 4b). Entrainment of water from the pycnocline was accompanied by an increase in surface nitrate concentration (Figure 4c). This picture is consistent with the classical interpretation of the storm's influence on the upper ocean: thinning of the pycnocline due to high-turbulence production at the base of the mixed layer and corresponding intrusion of nutrients. Supply of nutrients during the storm could be also driven by wind-generated inertial oscillation and associated shear instabilities across the pycnocline. Unfortunately, the

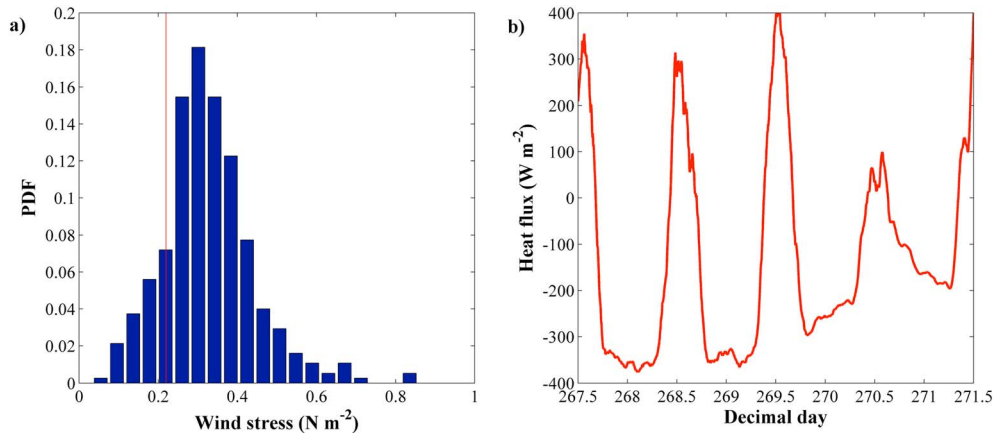


Figure 5. Wind stress and surface heat flux data during the observed storm event. (a) Histogram of wind stress values throughout the storm. The red vertical line indicates the critical wind stress (τ_{cr}) described in section 3.2. (b) Surface net heat flux from the ocean to the atmosphere during the storm event that occurred in the course of D381 cruise. The components of the net heat flux were calculated using meteorological data obtained on the cruise applying TOGA COARE 2.0 algorithm [Fairall et al., 1996]. The negative heat flux indicates the heat loss by the ocean.

quality of ADCP data during high wind forcing did not allow clear detection of shear spikes at the ocean pycnocline throughout the storm event. Hence, changes in surface nitrate concentrations during the storm may be the combined effect of both processes.

Meteorological data indicate that high wind speeds were accompanied by a significant decrease in the air temperature, by 2.5°C. To determine if vertical mixing during the storm was dominated by buoyancy reduction due to cooling or by shear production associated with wind mixing, the Monin-Obukhov length scale [Monin and Obukhov, 1954] was used:

$$L_{MO} = -\frac{u_*^3}{k_{vK} B} \quad (5)$$

where $k_{vK}=0.41$ is the von Karman constant, B is the surface buoyancy flux, $u_* = \left(\frac{\tau_w}{\rho_0}\right)^{1/2}$ is the friction velocity, $\rho_0 = 1026 \text{ kg m}^{-3}$ is the reference density, and τ_w is the wind stress. Above the Monin-Obukhov length scale shear production of turbulent kinetic energy dominates over buoyant reduction. If the length scale is deeper than the mixed layer depth, turbulence within the surface layer is mainly driven by wind forcing rather than convection [Nagai et al., 2005].

Combined National Centers for Environmental Prediction reanalysis and meteorological data obtained for the cruise period suggests that the net heat flux from the ocean to the atmosphere, Q , was at a minimum of -375 W m^{-2} during the storm (Figure 5b). The components of the net heat flux were calculated using the Tropical Ocean–Global Atmosphere (TOGA) Coupled Ocean–Atmosphere Response Experiment (COARE) 2.0 algorithm [Fairall et al., 1996]. Neglecting effects of evaporation and precipitation, the buoyancy flux can be estimated as

$$B = \frac{g\alpha Q}{\rho_0 c_p} \quad (6)$$

where $g=9.81 \text{ m s}^{-2}$ is the acceleration due to gravity, $\alpha=2.1 \times 10^{-4} \text{ }^\circ\text{C}^{-1}$ is the coefficient of thermal expansion for seawater, and $c_p=3985 \text{ J kg}^{-1} \text{ }^\circ\text{C}^{-1}$ is the seawater heat capacity (estimated for typical values of temperature and salinity within the mixed layer observed during the storm: $T \sim 14^\circ\text{C}$ and $S \sim 35.5$ practical salinity unit).

From equations (5) and (6), we estimated the weakest wind stress ($\tau_{cr} \sim 0.2 \text{ N m}^{-2}$) for which wind shear would be the main source of turbulence under the strongest convective conditions during the storm, assuming the mixed layer depth $\sim 40 \text{ m}$ (Figure 4b). Wind stress values during the storm were generally higher than τ_{cr} (Figure 5a). It suggests that turbulent kinetic energy production in the mixed layer and pycnocline erosion observed by Seagliders were mostly driven by wind forcing, rather than convection.

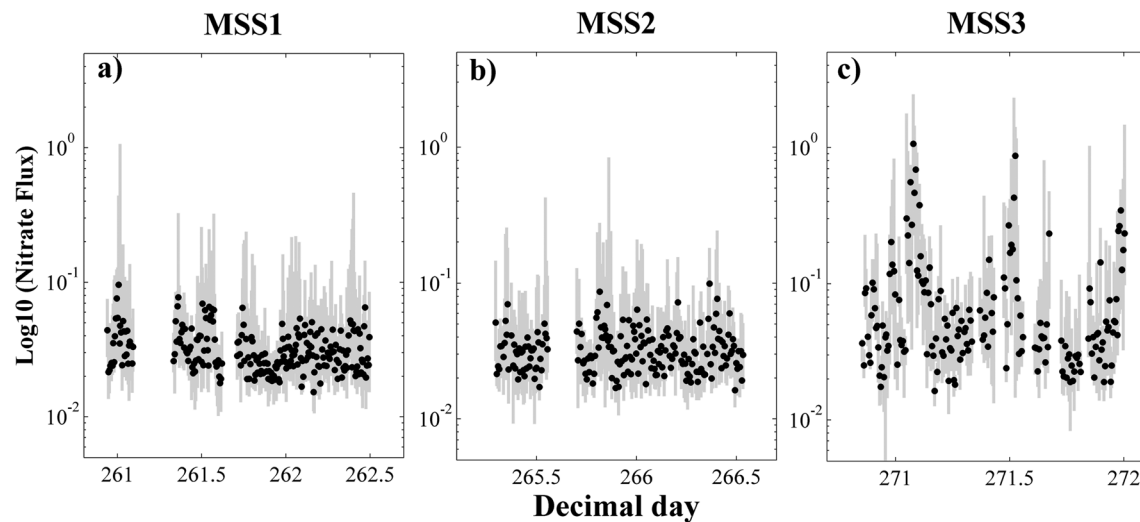


Figure 6. Vertical nitrate flux (y axis is in log scale; units are $\text{mmol N m}^{-2} \text{d}^{-1}$) through the pycnocline estimated from the three series of turbulence measurements: (a) MSS1, (b) MSS2, and (c) MSS3. The grey lines represent the interquartile range for each profile, and the black dots indicate the median values.

Following the passage of the storm, surface nitrate concentrations reached $\sim 0.6 \text{ mmol N m}^{-3}$. Multiplying the increase in concentration (by $\sim 0.5 \text{ mmol N m}^{-3}$ compared to the prestorm values) by the mixed layer depth ($\sim 40 \text{ m}$), nutrient supply due to the storm was estimated as $\sim 20 \text{ mmol N m}^{-2}$. The storm lasted about 3 days. Therefore, an increase in mixed layer nitrate by 20 mmol N m^{-2} is equivalent to a nitrate flux of $6\text{--}7 \text{ mmol N m}^{-2} \text{d}^{-1}$.

3.3. Shear Spiking After the Storm

Turbulence measurements conducted before and after the storm allowed us to estimate the additional supply of nutrients that could occur in the wake of the storm due to the presence of inertial currents in the surface layer and associated shear-spiking mechanism. During the prestorm period two series of turbulence measurements (MSS1 and MSS2) were conducted, providing estimates of the nitrate flux associated with background turbulent diffusion (Figure 4a). The third series of turbulence measurements (MSS3) took place immediately after the storm event, capturing interactions between wind stress and inertial currents which affected the magnitude and structure of the turbulent flux. According to the Seaglider data, the base of the euphotic zone was located within the pycnocline (Figures 3b and 4b). Therefore, we assumed that the nitrate flux through the pycnocline represented the flux into the euphotic zone. The nitrate flux was calculated for all 1 m bins within the pycnocline layer. To reduce the influence of outliers, only data points within the interquartile range were considered for each vertical profile.

For the prestorm turbulence measurements, MSS1 and MSS2, the nitrate flux was relatively constant (Figures 6a and 6b). The two series gave consistent estimates of the background turbulent diffusive nitrate flux: $0.04 \pm 0.03 \text{ mmol N m}^{-2} \text{d}^{-1}$. Poststorm (MSS3), three bursts of high nitrate flux (up to $1 \text{ mmol N m}^{-2} \text{d}^{-1}$, 32 times the standard deviations for MSS1 and MSS2) were observed (Figure 6c). The duration of the bursts was relatively short ($O(1 \text{ h})$). The time intervals between them were 10.7 and 11 h. The overall mean flux during MSS3 was $0.11 \pm 0.18 \text{ mmol N m}^{-2} \text{d}^{-1}$, approximately 3-fold higher than prestorm (MSS1 and MSS2).

The data suggest that the variability of the nitrate flux measured during MSS3 was affected by the poststorm inertial currents (Figure 7). At the beginning of MSS3 (days 270.9–271.6), the ADCP data captured rotation of the bulk shear vector at near the local inertial frequency ($\sim 15 \text{ h}$; Figure 7d). The magnitude of the bulk shear oscillated between 0.5 and $2 \times 10^{-5} \text{ s}^{-2}$ during this time (Figure 7b). By day 271.6 slab motion of the surface layer dissipated and the bulk shear value reduced (Figures 7b and 7d). The wind direction remained relatively constant throughout (Figure 7d). According to the theoretical model (equation (3)), the contribution of wind to shear production can be assessed by looking at the time series $|\vec{T}_w| \cos(\vec{S}, \vec{T}_w)$ as this metric encompasses the influence of wind direction relative to the bulk shear as well as the influence of wind magnitude. The time

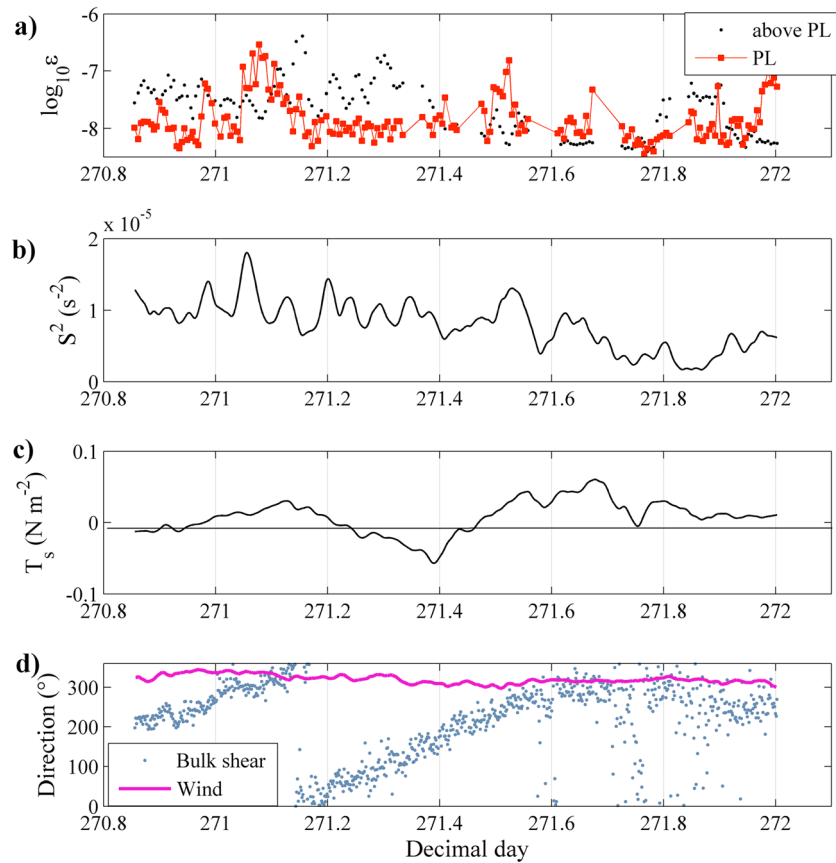


Figure 7. Forcing, shear, and turbulence characteristics during MSS3 transect during which the bursts of turbulent flux were observed: (a) decimal logarithm of median energy dissipation rate ϵ (units of ϵ are $\text{m}^2 \text{s}^{-3}$) within the pycnocline (red squares) and within the 10 m layer above the pycnocline (grey dots), (b) time series of bulk shear magnitude smoothed using 2 h boxcar filter, (c) wind stress magnitude multiplied by the cosine between wind and bulk shear directions, and (d) directions of wind stress (purple line) and bulk shear (blue dots).

series reveals that wind-supported shear production (i.e., $|\vec{T}_w| \cos(\vec{S}, \vec{T}_w) > 0$) occurred during days 271–271.2, 271.45–271.75, and at the end of the period of microstructure sampling when the inertial currents dissipated (Figure 7c). In agreement with the theory, the bursts of high mixing across the pycnocline occurred during these three periods and were associated with the enhanced bulk shear ($S^2 > 10^{-5} \text{s}^{-2}$). During the bursts, energy dissipation rate (ϵ) within the pycnocline was at least an order of magnitude higher than the background levels and the mean ϵ in the 10 m layer above the pycnocline (Figure 7a). The latter indicates that it was unlikely that simple deepening of the mixed layer due to surface forcing initiated the spikes in vertical mixing across the pycnocline.

4. Discussion

Previous studies [Forryan *et al.*, 2012; Martin *et al.*, 2010; Painter *et al.*, 2014] have suggested that the contribution of small-scale diapycnal turbulent diffusion to the overall physical transport of nutrients to the ocean surface layer is relatively minor. However, enhancement of the turbulent flux through the pycnocline associated with wind-driven inertial oscillations has not been considered in previous nitrate budget calculations for the open ocean. Shear spikes are discrete features, and enhancement of the nitrate flux due to them could be missed if measurements do not resolve subinertial frequencies.

The data set presented here has allowed direct observation of changes in the turbulent nitrate flux caused by shear spiking following the storm event in the open North Atlantic Ocean. A sequence of pulses of high nitrate flux generated by a wind event longer than the inertial period was observed, in agreement with

the sensitivity analysis of the model for shear production presented in *Burchard and Rippeth* [2009]. This model suggests that the period of alignment corresponds to the period of maximum shear production. In the current study the spikes of vertical mixing across the pycnocline occurred during the alignment (the first and the third spikes) and before the alignment (the second spike). In this study it was shown that maximum shear production depends also on the wind magnitude variability and complete alignment is not necessary to produce spikes in vertical mixing across the pycnocline.

Estimates of the background nitrate flux due to turbulent diffusion ($\sim 0.04 \text{ mmol N m}^{-2} \text{ d}^{-1}$) were consistent with the previous similar estimates at the PAP site [*Martin et al.*, 2010]. During MSS3 a short-term increase in turbulent nitrate flux (approximately 25 times higher than the background levels) was observed with the mean daily nitrate flux ($\sim 0.11 \text{ mmol N m}^{-2} \text{ d}^{-1}$) being higher only by a factor of 3. The nitrate supply by the poststorm shear spiking was an order of magnitude lower than the estimated nitrate flux during the storm ($6\text{--}7 \text{ mmol N m}^{-2} \text{ d}^{-1}$, 2 orders of magnitude higher than the background flux). Thus, the contribution of the poststorm nitrate supply appears to be low due to the short duration of periods of enhanced nitrate flux, and nutrients were delivered to the surface layer mainly during the storm. High values of nitrate flux during enhanced wind forcing ($\sim 22 \text{ mmol N m}^{-2} \text{ d}^{-1}$, 17-fold higher than the background flux) were also reported in previous studies in shelf seas [*Williams et al.*, 2013].

Using the estimates presented in this study, it is worth comparing the storm-driven nutrient supply with other regional physical mechanisms of nutrient transport to the surface ocean. The contribution of winter convection to the nitrate budget of this area of the North Atlantic was previously estimated as between $504 \text{ mmol N m}^{-2} \text{ yr}^{-1}$ [*Martin et al.*, 2010] and $1000 \text{ mmol N m}^{-2} \text{ yr}^{-1}$ [*Williams and Follows*, 2003]. Thus, nutrient intrusion during the storm caused by vertical mixing (20 mmol N m^{-2}) corresponds to 2.5–5% of the total annual nitrate supply by deep winter convection. The PAP site is in the transition region between the mesotrophic subpolar gyre and the oligotrophic subtropical gyre [*Henson et al.*, 2009]. Mesoscale eddy pumping has been estimated to provide approximately $200 \text{ mmol N m}^{-2} \text{ yr}^{-1}$ for oligotrophic regions [*McGillicuddy et al.*, 1998; *Siegel et al.*, 1999]. However, in subpolar regions the vertical advection by mesoscale eddies can potentially act as a sink of nutrients [*McGillicuddy et al.*, 2003; *Oschlies*, 2002b]. Hence, the magnitude, if not sign, of the mesoscale nitrate flux at the study site is uncertain. One instance of the effect of submesoscale filaments on primary production at the PAP site was reported by *Painter et al.* [2010], who showed that rates of primary production associated with the passage of an eddy filament could be highly variable with a potential increase of up to $74 \text{ mmol C m}^{-2} \text{ d}^{-1}$. Assuming a C:N ratio of 6.6 [*Redfield*, 1958] and a lifetime for a submesoscale front of $O(1)$ day [*Lévy et al.*, 2012], the total nitrate supply associated with this filament to support the primary production increase would be 11 mmol N m^{-2} . This is approximately one half of the nitrate associated with the storm pathway. However, estimates provided by *Painter et al.* [2010] are relevant for a single filament observed at the PAP site. In general, submesoscale fronts are ubiquitous features and collectively could be associated with higher nitrate flux.

One can make the point that storms in the high-latitude North Atlantic Ocean are localized features compared to basin-wide mechanisms of nutrient supply such as winter convection. However, the spatial scale of storms is relatively large ($O(100\text{--}1000)$ km) and comparable to the characteristic scale of the basin ($O(1000)$ km). Their passage is also fairly frequent: model-based estimates of storminess suggest that annually ~ 30 storms (with maximum wind speed $> 17 \text{ m s}^{-1}$) occur in the extratropical northeast Atlantic Ocean [*Weisse et al.*, 2005], although the majority of these storms occur in winter. We looked at the data from the weather mooring deployed at the PAP site from the end of April to November 2013, the time of year when surface nitrate is likely depleted. The data showed that during that period of time up to six low-pressure systems separated by several days with instantaneous wind speed exceeding 17 m s^{-1} passed through the site. A coarse estimate based on the results of the current study suggests that cumulative effects of these storm events can reach up to 30% of the nitrate supply by winter convection.

Previous studies estimated the impact of tropical cyclones on primary production in the North Atlantic Ocean using satellite ocean color data and obtained contradictory conclusions on their importance [*Foltz et al.*, 2015; *Hanshaw et al.*, 2008]. In this paper we have assessed the potential significance of extratropical storms for primary production in the high-latitude North Atlantic Ocean by focusing on nutrient supply. This study shows that on an annual scale the passage of storms can potentially support a significant amount of

ocean primary production and highlights the importance of further observational and modeling studies of storm contribution to nutrient supply in the ocean surface layer.

5. Conclusions

Based on the interdisciplinary data set collected at the Porcupine Abyssal Plain Sustained Observatory site we estimated nutrient fluxes to the ocean surface layer associated with the passage of a storm. Our observations demonstrated that the majority of nutrients were delivered to the mixed layer during the period of strong wind forcing. The turbulence measurements conducted in the wake of a storm allowed quantification of the additional poststorm nitrate flux due to the shear-spiking mechanism. Regardless of the dramatic semidiurnal increase of the flux, the overall nitrate supply after the storm was relatively low due to the short duration of the periods of enhanced mixing across the pycnocline. The estimate of the cumulative nitrate supply suggests that storms can form an appreciable component of the local annual nitrate budget.

Acknowledgments

The authors would like to thank L. Brannigan, M. Toberman, G. Damerell, K. Heywood, A. Thompson, J. Kaiser, V. Hemsley, M. Stinchcombe, the crew of RRS Discovery for their help with the data collection and processing, and two anonymous reviewers for their constructive comments, which helped us to improve the manuscript. OSMOSIS project was supported by NERC grant NE/I020083/1. A. Romyantseva was funded by a University of Southampton PhD studentship. The data set used in this study will be lodged with the British Oceanographic Data Centre (enquiries@bodc.ac.uk). In memory of Timothy Boyd.

References

- Babin, S. M., J. A. Carton, T. D. Dickey, and J. D. Wiggert (2004), Satellite evidence of hurricane-induced phytoplankton blooms in an oceanic desert, *J. Geophys. Res.*, *109*, C03043, doi:10.1029/2003JC001938.
- Brannigan, L., Y.-D. Lenn, T. P. Rippeth, E. McDonagh, T. K. Chereskin, and J. Sprintall (2013), Shear at the base of the oceanic mixed layer generated by wind shear alignment, *J. Phys. Oceanogr.*, *43*(8), 1798–1810, doi:10.1175/JPO-D-12-0104.1.
- Burchard, H., and T. Rippeth (2009), Generation of bulk shear spikes in shallow stratified tidal seas, *J. Phys. Oceanogr.*, *39*(4), 969–985, doi:10.1175/2008JPO4074.1.
- de Boyer Montégut, C., G. Madec, A. S. Fischer, A. Lazar, and D. Iudicone (2004), Mixed layer depth over the global ocean: An examination of profile data and a profile-based climatology, *J. Geophys. Res.*, *109*, C12003, doi:10.1029/2004JC002378.
- Fairall, C. W., E. F. Bradley, D. P. Rogers, J. B. Edson, and G. S. Young (1996), Bulk parameterization of air-sea fluxes for Tropical Ocean-Global Atmosphere Coupled-Ocean Atmosphere Response Experiment, *J. Geophys. Res.*, *101*, 3747–3764, doi:10.1029/95JC03205.
- Findlay, H. S., A. Yool, M. Nodale, and J. W. Pitchford (2006), Modelling of autumn plankton bloom dynamics, *J. Plankton Res.*, *28*(2), 209–220, doi:10.1093/plankt/fbi114.
- Foltz, G. R., K. Balaguru, and L. Ruby Leung (2015), A reassessment of the integrated impact of tropical cyclones on surface chlorophyll in the western subtropical North Atlantic, *Geophys. Res. Lett.*, *42*, 1158–1164, doi:10.1002/2015GL063222.
- Forryan, A., A. P. Martin, M. A. Srokosz, E. E. Popova, S. C. Painter, and M. C. Stinchcombe (2012), Turbulent nutrient fluxes in the Iceland Basin, *Deep Sea Res., Part I*, *63*, 20–35, doi:10.1016/j.dsr.2011.12.006.
- Hanshaw, M. N., M. S. Lozier, and J. B. Palter (2008), Integrated impact of tropical cyclones on sea surface chlorophyll in the North Atlantic, *Geophys. Res. Lett.*, *35*, L01601, doi:10.1029/2007GL031862.
- Henson, S. A., J. P. Dunne, and J. L. Sarmiento (2009), Decadal variability in North Atlantic phytoplankton blooms, *J. Geophys. Res.*, *114*, C04013, doi:10.1029/2008JC005139.
- Johnston, T. M. S., and D. L. Rudnick (2009), Observations of the transition layer, *J. Phys. Oceanogr.*, *39*, 780–797, doi:10.1175/2008JPO3824.1.
- Kirkwood, D. S. (1996), *Nutrients: Practical Notes on Their Determination in Seawater*, ICES Tech. Mar. Environ. Sci. Rep., vol. 17, 25 pp., International Council for the Exploration of the Seas, Copenhagen.
- Lampitt, R. S., D. S. M. Billett, and A. P. Martin (2010), The sustained observatory over the Porcupine Abyssal Plain (PAP): Insights from time series observations and process studies, *Deep Sea Res., Part II*, *57*(15), 1267–1271, doi:10.1016/j.dsr2.2010.01.003.
- Large, W. G., J. Morzel, and G. B. Crawford (1995), Accounting for surface wave distortion of the marine wind profile in low-level ocean storms wind measurements, *J. Phys. Oceanogr.*, *25*, 2959–2971, doi:10.1175/15200485.
- Lenn, Y., T. Rippeth, C. Old, S. Bacon, I. Polyakov, V. Ivanov, and J. Hølemann (2011), Intermittent intense turbulent mixing under ice in the Laptev Sea continental shelf, *J. Phys. Oceanogr.*, *41*(3), 531–547, doi:10.1175/2010JPO4425.1.
- Lévy, M., R. Ferrari, P. J. S. Franks, A. P. Martin, and P. Rivière (2012), Bringing physics to life at the submesoscale, *Geophys. Res. Lett.*, *39*, L14602, doi:10.1029/2012GL052756.
- Marra, J., R. Bidigare, and T. Dickey (1990), Nutrients and mixing, chlorophyll and phytoplankton growth, *Deep-Sea Res., Part A*, *37*(1), 127–143, doi:10.1016/0198-0149(90)90032-Q.
- Martin, A. P., and K. J. Richards (2001), Mechanisms for vertical nutrient transport within a North Atlantic mesoscale eddy, *Deep Sea Res., Part II*, *48*(4), 757–773, doi:10.1016/S0967-0645(00)00096-5.
- Martin, A. P., M. I. Lucas, S. C. Painter, R. Pidcock, H. Prandke, H. Prandke, and M. C. Stinchcombe (2010), The supply of nutrients due to vertical turbulent mixing: A study at the Porcupine Abyssal Plain study site in the northeast Atlantic, *Deep Sea Res., Part II*, *57*(15), 1293–1302, doi:10.1016/j.dsr2.2010.01.006.
- McGillicuddy, D., A. Robinson, D. Siegel, H. Jannasch, R. Johnson, T. Dickey, J. McNeil, A. Michaels, and A. Knap (1998), New evidence for the impact of mesoscale eddies on biogeochemical cycling in the Sargasso Sea, *Nature*, *394*, 263–266.
- McGillicuddy, D., L. Anderson, S. Doney, and M. Maltrud (2003), Eddy-driven sources and sinks of nutrients in the upper ocean: Results from a 0.1 resolution model of the North Atlantic, *Global Biogeochem. Cycles*, *17*(2), 1035, doi:10.1029/2002GB001987.
- Monin, A., and A. Obukhov (1954), Basic laws of turbulent mixing in the surface layer of the atmosphere, *Contrib. Geophys. Inst. Acad. Sci. USSR*, *151*, 163–187.
- Nagai, T., H. Yamazaki, H. Nagashima, and L. Kantha (2005), Field and numerical study of entrainment laws for surface mixed layer, *Deep Sea Res., Part II*, *52*(9), 1109–1132, doi:10.1016/j.dsr2.2005.01.011.
- Osborn, T. (1980), Estimates of the local rate of vertical diffusion from dissipation measurements, *J. Phys. Oceanogr.*, *10*(1), 83–89, doi:10.1175/1520-0485(1980)010<0083:EOTLRO>2.0.CO;2.
- Oschlies, A. (2002a), Nutrient supply to the surface waters of the North Atlantic, *J. Geophys. Res.*, *107*(C5), 3046, doi:10.1029/2000JC000275.
- Oschlies, A. (2002b), Can eddies make ocean deserts bloom?, *Global Biogeochem. Cycles*, *16*(4), 1106, doi:10.1029/2001GB001830.
- Painter, S. C., R. E. Pidcock, and J. T. Allen (2010), A mesoscale eddy driving spatial and temporal heterogeneity in the productivity of the euphotic zone of the northeast Atlantic, *Deep Sea Res., Part II*, *57*(15), 1281–1292, doi:10.1016/j.dsr2.2010.01.005.

- Painter, S., S. Henson, A. Forryan, S. Steigenberger, J. Klar, M. Stinchcombe, N. Rogan, A. Baker, E. P. Achterberg, and C. Moore (2014), An assessment of the vertical diffusive flux of iron and other nutrients to the surface waters of the subpolar North Atlantic Ocean, *Biogeosciences*, *11*, 2113–2130, doi:10.5194/bgd-10-18515-2013.
- Pelegrí, J. L., A. Marrero-Díaz, and A. Ratsimandresy (2006), Nutrient irrigation of the North Atlantic, *Prog. Oceanogr.*, *70*(2), 366–406, doi:10.1016/j.pocean.2006.03.018.
- Pollard, R. (1980), Properties of near-surface inertial oscillations, *J. Phys. Oceanogr.*, *10*(3), 385–398, doi:10.1175/1520-0485(1980)010<0385: PONSIO>2.0.CO;2.
- Redfield, A. C. (1958), The biological control of chemical factors in the environment, *Am. Sci.*, *46*, 205–221.
- Rippeth, T. P., M. R. Palmer, J. H. Simpson, N. R. Fisher, and J. Sharples (2005), Thermocline mixing in summer stratified continental shelf seas, *Geophys. Res. Lett.*, *32*, L05602, doi:10.1029/2004GL022104.
- Rippeth, T. P., P. Wiles, M. R. Palmer, J. Sharples, and J. Tweddle (2009), The diapycnal nutrient flux and shear-induced diapycnal mixing in the seasonally stratified western Irish Sea, *Cont. Shelf Res.*, *29*(13), 1580–1587, doi:10.1016/j.csr.2009.04.009.
- Sabine, C. L., R. A. Feely, N. Gruber, R. M. Key, K. Lee, J. L. Bullister, R. Wanninkhof, C. S. Wong, D. W. R. Wallace, and B. Tilbrook (2004), The oceanic sink for anthropogenic CO₂, *Science*, *305*(5682), 367–371, doi:10.1126/science.1097403.
- Sharples, J., J. F. Tweddle, J. Mattias Green, M. R. Palmer, Y.-N. Kim, A. E. Hickman, P. M. Holligan, C. Moore, T. P. Rippeth, and J. H. Simpson (2007), Spring-neap modulation of internal tide mixing and vertical nitrate fluxes at a shelf edge in summer, *Limnol. Oceanogr.*, *52*(5), 1735–1747, doi:10.4319/lo.2007.52.5.1735.
- Siegel, D. A., D. J. McGillicuddy, and E. A. Fields (1999), Mesoscale eddies, satellite altimetry, and new production in the Sargasso Sea, *J. Geophys. Res.*, *104*(C6), 13,359–13,379, doi:10.1029/1999JC900051.
- Son, S., T. Platt, H. Bouman, D. Lee, and S. Sathyendranath (2006), Satellite observation of chlorophyll and nutrients increase induced by Typhoon Megi in Japan/East Sea, *Geophys. Res. Lett.*, *33*, L05607, doi:10.1029/2005GL025065.
- Weisse, R., H. von Storch, and F. Feser (2005), Northeast Atlantic and North Sea storminess as simulated by a regional climate model during 1958–2001 and comparison with observations, *J. Clim.*, *18*(3), 465–479, doi:10.1175/JCLI-3281.1.
- Williams, C., J. Sharples, C. Mahaffey, and T. Rippeth (2013), Wind-driven nutrient pulses to the subsurface chlorophyll maximum in seasonally stratified shelf seas, *Geophys. Res. Lett.*, *40*, 5467–5472, doi:10.1002/2013GL058171.
- Williams, R. G., and M. J. Follows (2003), Physical transport of nutrients and the maintenance of biological production, in *Ocean Biogeochemistry: A JGOFS Synthesis*, edited by M. Fasham, 19–50, Springer, New York.
- Williams, R. G., A. J. McLaren, and M. J. Follows (2000), Estimating the convective supply of nitrate and implied variability in export production over the North Atlantic, *Global Biogeochem. Cycles*, *14*(4), 1299–1313, doi:10.1029/2000GB001260.
- Wu, Y., T. Platt, C. C. Tang, S. Sathyendranath, E. Devred, and S. Gu (2008), A summer phytoplankton bloom triggered by high wind events in the Labrador Sea, July 2006, *Geophys. Res. Lett.*, *35*, L10606, doi:10.1029/2008GL033561.